Studies on the structural, optical and electrical properties of Nb doped TiO_2 nanostructured thin films

A. T. RAJAMANICKAM*, P. THIRUNAVUKKARASU[a], K. DHANAKODI[b]
Department of Electronics and Communication System, Nehru Arts and Science college, Coimbatore -641 105, Tamilnadu, India
[a]*Department of Electronics, SRMV College of Arts and Science, Coimbatore -641 120, Tamilnadu, India*
[b]*Department of Electronics, KSG College of Arts and Science, Coimbatore - 641 015, Tamilnadu, India*

Niobium (Nb) doped TiO_2 thin films were synthesized by simple chemical bath deposition method. The influence of Nb doping on structural, optical, electrical and morphology of thin films were studied by X-ray diffraction (XRD), Fourier Transform Infrared Spectra (FTIR), UV-Vis Spectra, photoluminescence (PL), four point probe mode and AFM images. X-ray diffraction (XRD) results showed that both pristine and Nb (5 wt%) films formed mixture of anatase (A) and rutile (R) type phase. The surface roughness has been found to decrease with the increase of the dopant concentration as investigated by atomic force microscopy. Optical studies showed that the energy band gap of the films was lowered from 3.32 eV to 3.13 eV on Niobium (Nb) doping. PL emission intensity was decrease with Nb doped samples, which confirm the Nb doping in to TiO_2 host lattice site. The electrical resistivity was found to be 0.9185 Ω.cm and 0.6125 Ω.cm for pristine and Nb doped TiO_2 films for 500°C. This result confirmed that Nb doping has strong influence in the electrical properties of pure TiO_2.

(Received January 03, 2015; accepted February 10, 2016)

Keywords: Transparent Conducting oxides, TiO_2 thin films, Nb doping, Optical property, Resistivity

1. Introduction

Transparent conducting oxides (TCOs) are a unique type of materials that combine electrical conductivity and optical transparency, simultaneously, with a wide range of applications e.g. displays, low emissive (low-e) windows, thin film photovoltaic (PV) and smart devices [1]. Titanium dioxide (TiO_2) belongs to the family of transition metal oxides. In nature, TiO_2 is known to occur in the structures of rutile, anatase, and brookite (brookite is a minority product of most synthesis). TiO_2 is a wide band gap semiconductor material which has been under extensive investigations due to its applications in a variety of fields such as dye-sensitized solar cell [2], gas sensors [3], photocatalysts [4-5], wave guiding [6], antireflective coatings [7], dielectric [8], etc. Tin-doped indium oxide (ITO) is a widely used material for TCO applications due to its high transmittance to visible light and high conductivity, but it is so important to find a substitute for it because of indium natural resources rarity. Although in recent years aluminum-doped zinc oxide (ZAO) [9] and fluorine-doped tin oxide (FTO) [10] are presented as new TCOs but the hardship in large area preparation of ZAO films with smooth surface morphology and easily etched ZAO films in both acid and alkaline environment and also relatively low electrical conductivity of FTO and its difficulty to pattern via wet etching as compared to ITO [11] Furubayashi et al. [12] prepared the Nb-doped TiO_2 (TNO) thin film by pulsed laser deposition (PLD) method and reported it as a novel TCO material with minimum resistivity of 2.3×10^{-4} Ω.cm and the transparency of higher than 95% in the visible range. Yamada et al. [13] also fabricated highly conductive polycrystalline TNO film on glass substrate by sputtering method so that resistivity of the film was measured 3×10^{-4} Ω.cm at room temperature and optical transmittance was achieved 75% in the visible range. Although highly conductive and transparent TNO thin films can be obtained by above methods, but industrial productions are limited by the expensive vacuum technique. Furthermore, the homogeneous and large-area films preparation is also an upfront challenge yet. A chemical bath deposition method has several advantages including simplicity, low cost, easily controlled doping levels and feasible preparation of large area films. Moreover the method is simple, less time consuming and cost effective compared to other methods. Moreover sufficient degree of crystallinity is required to attain the desired electronic properties necessary for photocatalytic applications. This can be achieved through annealing the films (catalyst) materials at higher temperatures (500°C/2h) in ambient atmospheres. So in the present work consist of synthesis and systemic investigation of structural, optical and electrical properties of Nb doped TiO_2 thin films by using simple chemical bath deposition method.

2. Experimental procedure

2.1 Preparation of Nb-TiO_2 thin films

Nb-TiO_2 thin films were prepared on carefully cleaned (in an ultrasonic water bath and then in absolute

ethanol) quartz glass substrates by chemical bath deposition technique. The starting solution was prepared by mixing of titanium isopropoxide, niobium (V) chloride ($NbCl_5$), ethyl alcohol in molar ratio 5:50, in a closed beaker stirred for 30 min pH of the sol was adjusted to 8 with the addition of 2 ml of NH_4OH. Distilled water (1.5 mol) was added and the solution was refluxed under dry atmosphere for 2 h at 60 ºC. For completion of the hydrolysis process, the solution was kept stirred at room temperature for overnight. The substrate was suspended vertically in the reaction bath after stirring the solution properly for homogeneity. The thin film samples were deposited at room temperature for 1 h. The as-deposited thin films were annealed at 500 ºC for 2 h in muffle furnace, in order to improve the crystanility. Pure TiO_2 thin films were prepared in a similar manner without the use of niobium source.

2.2 Characterization techniques

The prepared samples (annealed) were successfully characterized by the following techniques. Structural properties of the Nb-TiO_2 thin films are analyzed using X-ray diffraction (XRD, JEOL diffractometer) with monochromatized Cu Kα radiation (λ=1.54056 Å) in range of 10-80˚ with step size of 0.1˚ and the Fourier transform infrared (FT-IR) spectra are recorded on a Shimadzu-8400S spectrometer in range of 400 - 4000 cm^{-1} using KBr pellets. The optical transmittance is measured by UV–Vis spectrophotometer (JASCO V-500) in the wavelength range of 300 - 900 nm. For electrical conductivity, the sheet resistance values of the films are recorded by a Jandel four point surface resistivity meter (RM3-AR) at room temperature. The morphology of the Nb-TiO_2 thin films is observed by scanning electronic microscope (JEOL Model JSM – 6390LV). Photoluminescence spectra of the samples were recorded using PerkinElmer LS 55 Spectrometer equipped with a 40 W Xenon lamp, Excitation length used was 325 nm.

3. Results and discussion

3.1 XRD analysis

Non-destructive X ray diffraction technique was used to determine the phase crystallinity and structural analysis of the pure and Nb doped TiO_2 thin films as shown in Fig. 1. It can be seen that the diffraction peaks of both samples are ascribed to the peaks of anatase and rutile phase. The observations indicate that there is no phase change in TiO_2 during the doping process. It was also noted that the XRD peak intensity decreases for Nb doped TiO_2, which indicating the growth is suppressed due to Nb doping. The lattice parameters of pristine TiO_2 were estimated as a = b = 4.594 (Å) and c = 2.967 (Å). These values decrease to a = b = 4.484 (Å) and c = 2.878 (Å) after Nb doping (Table 1). The observed variation in lattice parameters is consistent with the smaller radius of the Nb^{5+} ion (0.64 Å) with respect to the Ti^{4+} ion radius (0.68 Å) and with the small amount of Nb concentration used for doping.

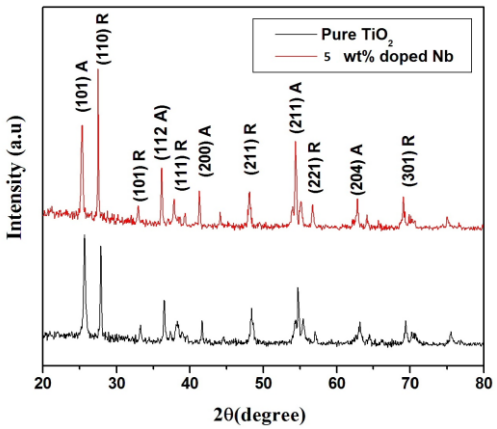

Fig. 1. XRD pattern of pure and Nb (5 wt.%) doped TiO_2 thin films.

The average crystalline sizes of the Nb-TiO_2 thin films were calculated by using Scherrer's equation [14].

$$d = \frac{K\lambda}{\beta \cos\theta}$$

where d is the mean crystallite size, K is the shape factor taken as 0.89, λ is the wavelength of the incident beam, β is the full width at half maximum and θ is the Bragg angle. The average crystalline size of TiO_2 was found to be 25 nm and it was further decrease to 19 nm for 5 wt % Nb doped TiO_2 thin films. This decrease in grain size of TiO_2 suggests that the growth is concealed due to doping of Nb into Ti-site.

Table 1. Lattice parameter and crystallite size of pure and Nb doped TiO_2 thin fims.

Samples	Crystallite Size (nm)	Lattice Parameters a(Å)	c(Å)	Volume ($Å^3$)
TiO_2	25	4.594	2.967	62.61
Nb-TiO_2	19	4.584	2.878	60.47

3.2 Scanning electron microscope analysis

Scanning electron microscopy (SEM) is a useful technique to determine the surface morphology and particle size of the samples. Fig. 2 shows the SEM image of pure and Nb doped TiO_2 thin films. The microstructure of Nb-TiO_2 consisting of many spherical shaped crystalline particles. It can be seen that the surface of the films are very smooth and the crystalline size are fine. There is no big particle found in the micrograph. The average grain size of pure TiO_2 was found to be 28 nm, further it was decrease to 20 nm for Nb doped TiO_2 thin films. This result confirms that Nb doping has significant

influence in the TiO_2 film surface structure.The average crystalline size of TiO_2 was found to be 28 nm.

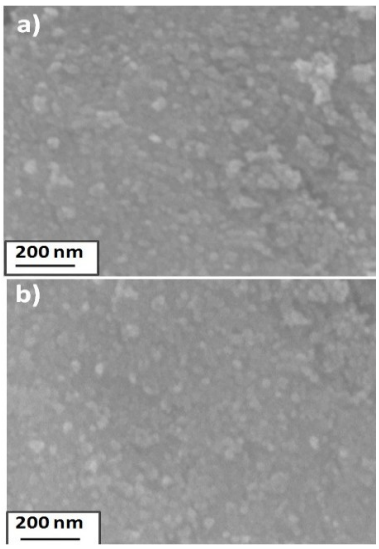

Fig. 2. SEM image of a) Pure TiO_2 b) Nb (5 wt.%) doped TiO_2 thin films.

3.3 AFM analysis

Atomic force microscopy (AFM) is a useful technique to determine the surface morphology and particle size of the samples. Figs. 3 shows the 2D and 3D AFM image of pure and Nb doped TiO_2 thin films. It was noted that the surface of the films were very smooth. The particles distribution is uniform and also particle size reduces for Nb doped samples when compared to pure TiO_2. For an optical surface, roughness is normally considered as an important parameter. Surface roughness not only the light scattering but also give an idea about the quality of the surface under investigation, in addition to providing some insight on the growth morphology. A systematic description of various analytical method used for roughness characterization can be found in ref [15].

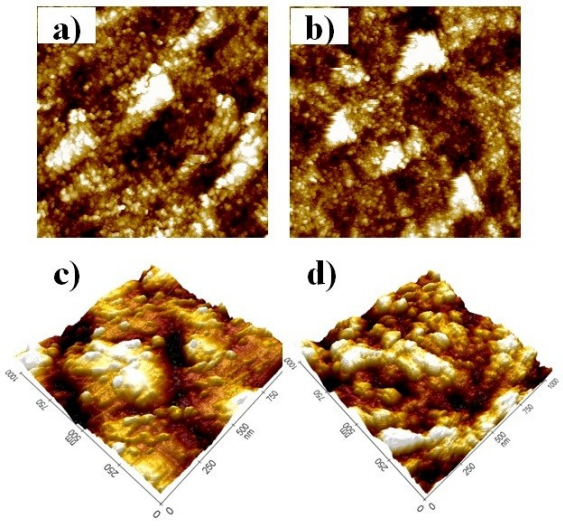

Fig. 3. AFM 2D image of a) Pure TiO_2 b) Nb (5 wt.%) doped TiO_2, 3D image of c) Pure TiO_2 d) Nb (5 wt.%) doped TiO_2 thin films.

The Rrms values of pristine and Nb doped TiO_2 were found to be 31, 22 nm respectively. These values are good in agreement with the crystalline size calculated from XRD results.

3.4 UV-Vis spectra analysis

In order to confirm the optical property and substitution of Nb in to TiO_2 site, the films were characterized by UV-Vis transmission spectra analysis. Fig. 4 a) show the UV-Vis transmission spectra analysis of pure and Nb doped TiO_2 films. Both the films are highly transparent in the visible region and a sharp fall in transmission is observed below 400 nm region. It is found that the absorption edge shifts toward longer wavelength (red shift) with doping of Nb ion. The observed red shift can be attributed to charge transfer transitions between localized d electrons of Nb ion and TiO_2 conduction band or valance band [16].

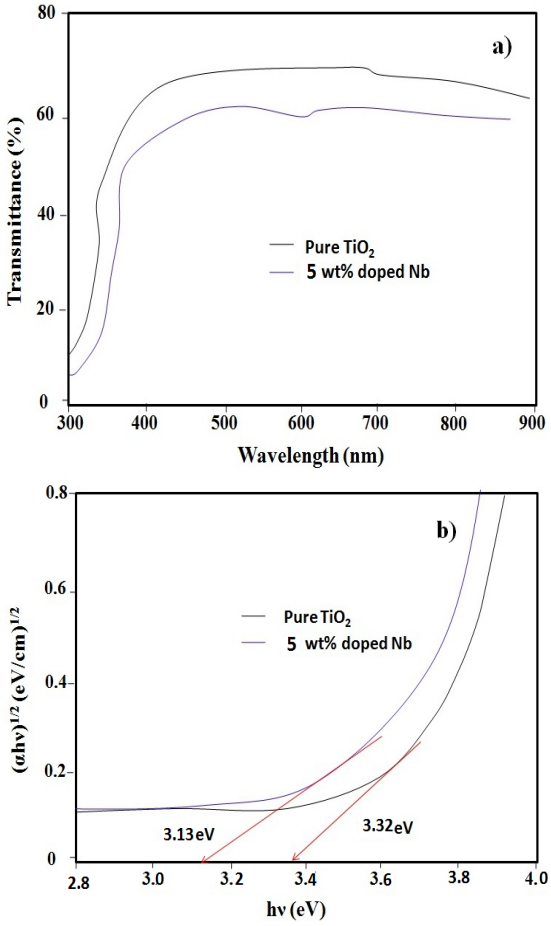

Fig. 4. UV-Vis spectra of a) Pure TiO_2 b) Nb (5 wt.%) doped TiO_2 thin films.

The absorption coefficient (α) was calculated from the transmission spectra using equation [17],

$$\alpha = 1/t \ln(1/T)$$

Where T is the optical transmission and t is the film thickness. The direct band gap of thin films were calculated from Figs. 4 b) using the formula [18],

$$\alpha h\nu = A(h\nu - E_g)^m$$

Where α is the absorption coefficient, h is the Planck's constant, ν is the frequency of incident light, E_g is the energy band gap of material and m is the factor governing the direct/indirect, etc. transition of electron from the valance band to the conduction band. The band gap energy was calculated as 3.32 eV and 3.13 eV for pure and Nb doped TiO_2 films. The observed decrease in band gap energy confirms that Nb^{5+} ion substituted in TiO_2 host lattice. Similar findings were observed in Fe doped TiO_2 thin films [19].

3.5 Photoluminescence spectra analysis

PL emission spectra have been widely used to investigate the efficiency of charge carrier trapping, migration and transfer, and to understand the fate of electron hole pairs in the semiconducting oxide materials [19]. Fig. 5 shows the PL emission spectra of both pure and Nb doped TiO_2 films measured from 300 to 600 nm using a 325 nm He–Cd laser. The pure TiO_2 samples show UV emission (395 nm), blue-green (425, 467 nm) and green emissions (490 nm) were observed at 415 and 490 nm respectively. We attributed the UV emission to dangling bond and structural defects. The broad blue emission to electron transition mediated by defect levels in the band gap, such as oxygen vacancies, Ti interstitials. After substitution of Nb^{5+} ion all the emission peak shifts a little to lower energy with decreased intensity. The incorporation Nb^{5+} ion in TiO_2 host lattice and decreasing the optical band gap energy was also confirmed by UV-VIS absorption spectroscopy. The green emission peak (490 nm) was related to V^{+}_{O} oxygen vacancies.

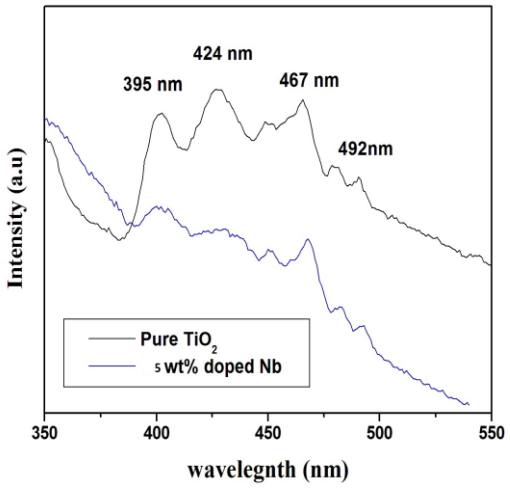

Fig. 5. Photoluminescence spectra of Pure and Nb (5 wt.%) doped TiO_2 thin films.

3.6 FTIR spectra analysis

Infra–red spectrum is an important record, which gives sufficient information about the structure and functional groups of a compound. Fourier transform infrared spectra of pure and Nb doped TiO_2 films are shown in fig. 6. From this spectrum, it clearly seen that strong band appeared in the range of 580 and 660 cm^{-1}, which is related to the characteristic modes of TiO_2. Generally, the IR absorption bands in the regions of 800–600 cm^{-1} can be attributed to anatase and rutile phases of TiO_2 [20]. The absorption bands between 3446.46 and at 1605.11 cm^{-1} are clearly seen, which are gradually decreased for Nb doped TiO_2. These bands are attributed to the stretching vibrations of the O-H groups and the bending vibrations of the adsorbed water molecules, respectively. The remaining low signals attributed to some OH groups at the surface were probably due to the re-absorption of water from the ambient atmosphere [21].

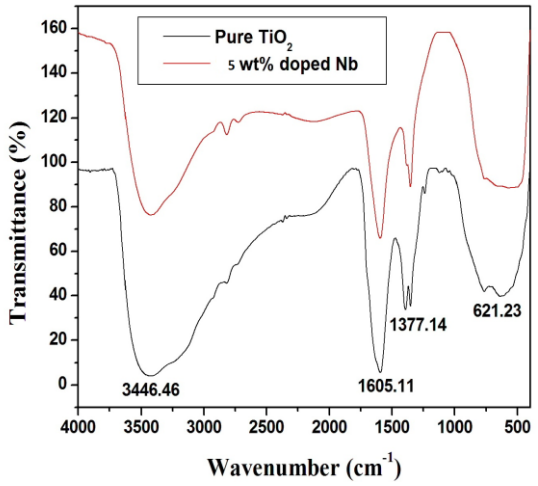

Fig. 6. FTIR spectra of Pure and Nb (5 wt.%) doped TiO_2 thin films

3.7 Electrical measurements

The electrical resistivity of the annealed films of both pure and Nb doped TiO_2 was determined in the temperature range from RT to 500°C by using four probe method (Scientific equipment, Roorkee, India) with ± 0.5 accuracy. The distance between the two probes was 0.3 cm and electrode contact was made using silver paste. Fig. 7 shows the electrical resistivity measurement of pure and Nb doped TiO_2 films as a function of temperature. The resistivity of pure TiO_2 was found to be 1.8 Ω.cm and 0.9185 Ω.cm for RT and 500°C respectively. The observed decrease in resistivity due to Ti^{4+} ions have more concentration in films obtained with high annealing temperature regarding the O^{2-} ions, which results in an increase in the free electron concentration there after there is a decrease in film's resistivity [22]. The resistivity of Nb doped TiO_2 was found to be 1.2 Ω.cm and 0.6125 Ω.cm for RT and 500°C respectively. The resistivity drastically

decreased for Nb doped TiO_2 films, because Nb-doped TiO_2 could exhibit a stronger n-type character and a higher electronic conductivity than undoped TiO_2 as the electron concentration in the titania lattice might increase and the Fermi level might be shifted closer to the conduction band level. The extracted bandgap values of the annealed TNO films slightly decreases from 3.32 eV to 3.13 eV, as shown in

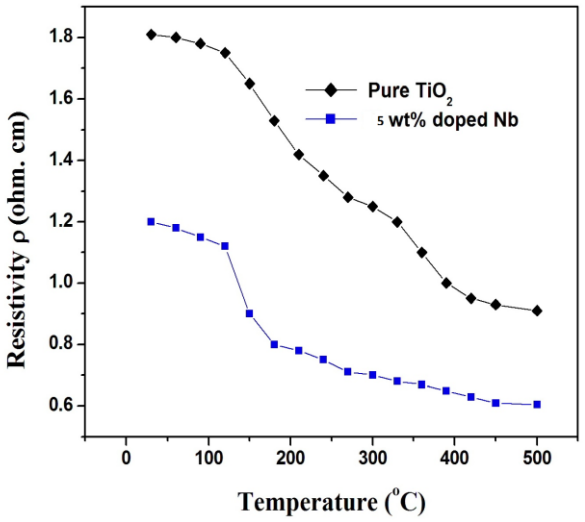

Fig. 7. Electrical Resistivity measurements of Pure and Nb (5 wt.%) doped TiO_2 thin films.

Fig. 8 on the other hand, the relative position of the Fermi level (E_C-E_F) drastically shifts up closer to the conduction band minimum, from 0.51 eV to 0.13 eV. The results, suggested that the n-type semiconducting behavior of Nb-doped TiO_2 is enhanced by inducing oxygen deficiency related to Nb^{5+} states, which additionally donate of free electrons to the formation of d-orbital conduction paths. The preliminary results obtain from the electrical measurements confirm that Nb doping has strong influence in the electrical properties of TiO_2 thin films and these films are more suitable for high performance gas sensor device.

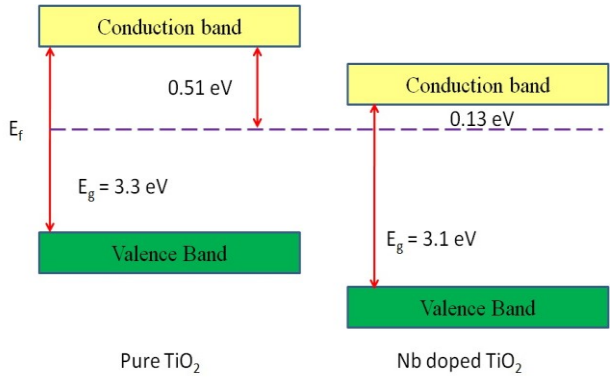

Fig. 8. Energy level diagram of Nb-TiO_2 thin films.

4. Conclusions

In summary, we have successfully synthesized Nb doped TiO_2 thin films by chemical bath deposition method. The diffraction peaks of both samples are ascribed to the anatase and rutile phase of TiO_2. The average crystalline size of TiO_2 was found to be 25 nm and it was further decrease to 19 nm for 5 wt % Nb doped TiO_2 thin films. The SEM micrograph of Nb-TiO_2 consisting of many spherical shaped crystalline particles. The surface of the films is very smooth and the uniform crystalline size. The surface roughness has been found to decrease with the increase of the dopant concentration as investigated by atomic force microscopy. A considerable red shift in the absorption edge was found to be Nb doped TiO_2 by UV-Vis absorption spectra. The functional groups were analyzed by using FTIR analysis. The defect in band gap energy and oxygen vacancy was analyzed by using PL emission spectra. The drastic decrease of resistivity or increase the conductivity of Nb doped TiO_2 confirm the Nb doping has significant improvement in the electrical properties of TiO_2 films. So these types of materials are preferable of gas sensing applications.

References

[1] D. S. Ginley, Handbook of transparent conductors, Springer, 2010.
[2] T. Antonio Otávio, Patrocínio, B. Eucler, Paniago, M. Roberto, Y. Paniago, Neyde, Murakami Iha, Appl. Surf. Sci., **254,** 1874 (2008).
[3] A. Ibrahim, J. S. Al-Homoudi, R. Thakur, G. W. Naik, G. Auner, Newaz, Appl. Surf. Sci., **253,** 8607 (2007).
[4] M. R. Hoffmann, S. T. Martin, W. Choi, D. W. Bahnemann, Chem. Rev., **95**, 69 (1995).
[5] X. Z. Li, H. Liu, L. F. Cheng, H. J. Tong, Sci. Tech., **37**, 3989 (2003).
[6] R. Mechiakh, F. Meriche, R. Kremer, R. Bensaha, B. Boudine, A. Boudrioua, Optical Mater. **30,** 645 (2007).
[7] Sang-Hun Jeong, Jae-Keun Kim, Bong-Soo Kim, Seok-Ho Shim, Byung-Teak Lee, Vacuum., **76**, 507 (2004).
[8] Wenli Yang, Colin A. Wolden, Thin Solid Films., **515,** 1708 (2007).
[9] X. Zi-qiang, D. Hong, L. Yan, C. Hang, Materials science in semiconductor processing, **9,** 132 (2005).
[10] E. Premalal, N. Dematage, S. Kaneko, A. Konno, Thin Solid Films, **520,** 6813 (2012).
[11] H. Liu, V. Avrutin, N. Izyumskaya, U. Ozgur, H. Morkoc, Superlattices and Microstructures **48,** 458 (2010).
[12] Y. Furubayashi, T. Hitosugi, Y. Yamamoto, K. Inaba, G. Kinoda, Y. Hirose, T. Shimada, T. Hasegawa, Appl. Phys. Lett. **86**, 252101 (2005).
[13] N. Yamada, T. Hitosugi, J. Kasai, N. L. H. Hoang, S. Nakao, Y. Hirose, T. Shimada, T. Hasegawa, Thin Solid Films, **518,** 3101 (2010).

[14] M. Parthibavarman, K. Vallalperuman, S. Sathishkumar, M. Durairaj, K. Thavamani, Journal of Materials Science: Materials in Electronics**. 25,** 730 (2014).
[15] J. M. Bennett, L. Mattson, Introduction to Surface Roughness and Scattering, Optical Society of America, Washington, DC, 1989.
[16] A. Kubacka, G. Colo´n, M. Ferna´ndez-Garcı´a, Catalysis Today., **143**, 286 (2009).
[17] S. S. Roy, J. Podder Gilberto, J. Optoelect. Adv. M., **12**, 1479 (2010).
18] R. K. Nath, S. S. Nath, Journal of Analytical Science & Technology., **3**, 85 (2012).
[19] B. Prabitha, V. B. Nair, P. Justinvictor, Georgi, P. Daniel, K. Joy, V. Ramakrishnan, David Devaraj Kumar, P. V. Thomos, Thin solid Films., **550,** 121 (2014).
[20] B. M. Reddy, I. Ganesh, E. P. Reddy, A. Femandez, P. G. Smirniotis, Journal of Physical Chemistry B., **105**, 6227 (2001).
[21] Yung-Jen Lin, Ching-Jiunn Wu, Surface and Coating Technology. **88**, 239 (1997).
[22] M. A. Malati, W. K. Wong, W. K, Surface Technology, **22**, 305 (1984).

*Corresponding author: atrmanic@gmail.com